Origin of Spectral Purity and Tuning Sensitivity in a Spin Transfer Vortex Nano-Oscillator

A. Hamadeh,[1] N. Locatelli,[2] V. V. Naletov,[1,2,3] R. Lebrun,[2] G. de Loubens,[1*] J. Grollier,[2] O. Klein,[1,4] and V. Cros[2]
[1]Service de Physique de l'État Condensé (CNRS URA 2464), CEA Saclay, 91191 Gif-sur-Yvette, France
[2]Unité Mixte de Physique CNRS/Thales and Université Paris Sud 11, 1 Avenue Fresnel, 91767 Palaiseau, France
[3]Institute of Physics, Kazan Federal University, Kazan 420008, Russian Federation
[4]SPINTEC, UMR CEA/CNRS/UJF-Grenoble 1/Grenoble-INP, INAC, 38054 Grenoble, France
(Received 17 October 2013; published 25 June 2014)

We investigate the microwave characteristics of a spin transfer nano-oscillator (STNO) based on coupled vortices as a function of the perpendicular magnetic field $H_\perp$. Interestingly, we find that our vortex-based oscillator is quasi-isochronous independently of $H_\perp$ and for a dc current ranging between 18 and 25 mA. It means that the severe nonlinear broadening usually observed in STNOs can be suppressed on a broad range of bias. Still, the generation linewidth displays strong variations on $H_\perp$ (from 40 kHz to 1 MHz), while the frequency tunability in current remains almost constant (7 MHz/mA). This demonstrates that isochronicity does not necessarily imply a loss of frequency tunability, which is here governed by the current induced Oersted field. It is not sufficient either to achieve the highest spectral purity in the full range of $H_\perp$. We show that the observed linewidth broadenings are due to the excited mode interacting with a lower energy overdamped mode, which occurs at the successive crossings between harmonics of these two modes. These findings open new possibilities for the design of STNOs and the optimization of their performance.

DOI: 10.1103/PhysRevLett.112.257201 PACS numbers: 85.75.−d, 75.78.−n

A spin-polarized current exerts on a ferromagnetic material a torque that can compensate the damping and lead to auto-oscillation of the magnetization [1–4]. Owing to their tunability, agility, compactness, and integrability, spin transfer nano-oscillators (STNOs) are promising candidates for various high frequency applications such as frequency generation [5], signal processing [6], and microwave frequency detection [7]. They have also been proposed to increase the data transfer rate of read heads [8,9] and in microwave assisted magnetic recording [10]. More recently, they were even mentioned as components for innovative architectures such as associative memories [11]. From a more fundamental viewpoint, STNOs have also been useful to experimentally demonstrate interesting theoretical ideas such as the onset of chaos [12], "Devil's staircase" [13], or novel forms of magnetic solitons [14].

As far as microwave applications are concerned, spectral purity and tuning sensitivity are two key characteristics for STNOs. A particularity of such devices compared to other oscillators is their strong nonlinear properties, which are inherited from the equation of motion of magnetization [15]. On one hand, they confer interesting properties to STNOs, as for instance their large frequency tunability [4,16]. On the other hand, they lead to a severe broadening of the generation linewidth [17]: due to nonlinear phase-amplitude coupling, the phase noise of STNOs is indeed rather large [18,19], which is the main limiting factor to their practical applications. In this Letter, we shall demonstrate that strong nonlinearities are not necessary to achieve large tuning sensitivity, while minimizing nonlinearities is not sufficient to obtain high spectral purity, which points towards alternative routes to engineer STNOs with improved performance.

So far, some of the best microwave characteristics have been reported for STNOs in which spin transfer torque (STT) excites the gyrotropic mode of a magnetic vortex [20]. It results in microwave emission in the range from 100 MHz to 2 GHz, characterized by a narrow linewidth (about 1 MHz) and large output power in the case of tunnel junction devices [21]. Moreover, the oscillation frequency of vortex-based STNOs can be rapidly modified between different values using the bias current, which demonstrates their high agility and tunability in current [22]. Recently, we have reported a record high spectral purity (ratio of center frequency to full linewidth $> 15\,000$) in a spin-valve nanopillar where STT drives the dynamics of two coupled vortices (one in each ferromagnetic layer) [23]. In such a STNO, the generation linewidth at fixed dc current $I_{\rm dc}$ displays strong variations [down from 40 kHz [Fig. 1(a)] up to 1 MHz [Fig. 1(b)]] on the applied perpendicular field $H_\perp$, as displayed in Fig. 2(a). At the same time, its frequency tunability $dF/dI_{\rm dc} \simeq 7$ MHz/mA remains almost constant [see Fig. 2(b)], which points out that spectral purity and tuning sensitivity are not necessarily correlated. In the following, we aim at understanding the physical origin of these peculiar behaviors, as this will give hints to optimize the characteristics of STNOs.

The studied STNO is a circular nanopillar of diameter $2R = 250$ nm patterned from a (Cu60|Py_B15|Cu10|Py_A4|Au25) stack, where thicknesses are in nm

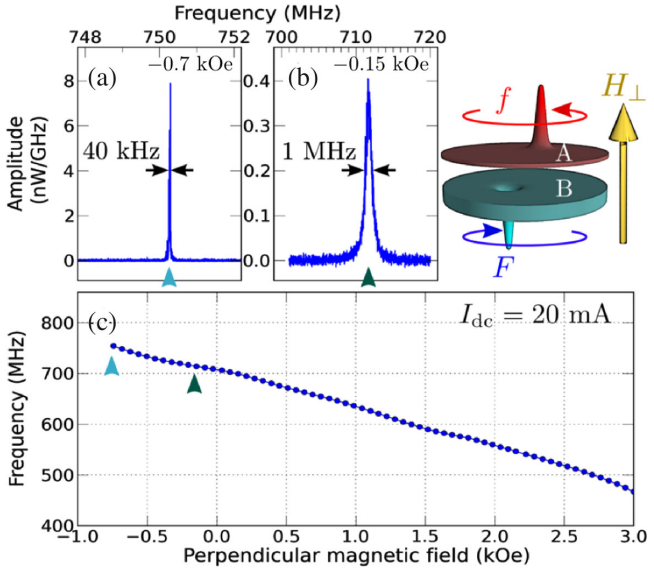

FIG. 1 (color online). Upper right sketch: STNO based on coupled vortices. (a) Power density spectra measured at $I_{dc} = 20$ mA and a perpendicular magnetic field $H_\perp = -0.7$ kOe and (b) $H_\perp = -0.15$ kOe. (c) Dependence of the fundamental oscillation frequency on $H_\perp$.

and Py $= Ni_{80}Fe_{20}$, which can sustain the double vortex configuration [23,24]. A current $I_{dc} > 0$ is injected through the STNO using the bottom Cu and top Au electrodes, which corresponds to electrons flowing from the thick Py_B to the thin Py_A layer. In both Py layers, the vortex chiralities are parallel to the orthoradial Oersted field produced by I_{dc}. We use a magnetic field $H_\perp$ perpendicular to the sample plane in order to control the relative orientation of the

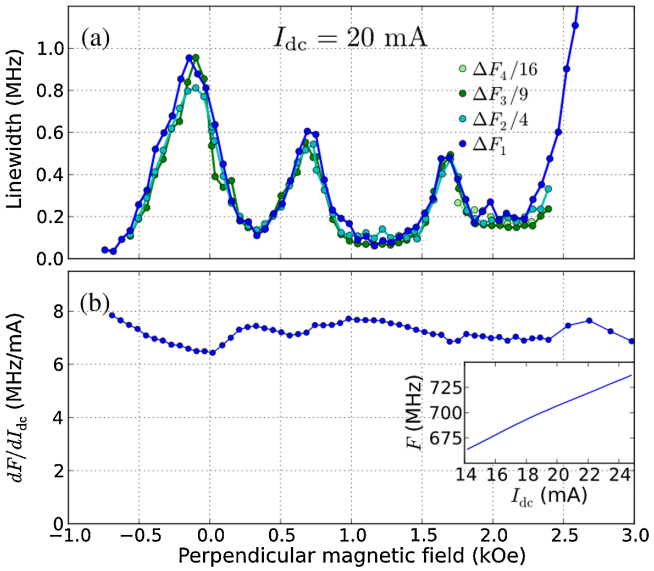

FIG. 2 (color online). (a) Generation linewidths of harmonics $n = 1$ to 4 divided by n^2 as a function of $H_\perp$. (b) Frequency tunability versus $H_\perp$. Inset: dependence of the oscillation frequency on I_{dc} measured at $H_\perp = 0$ kOe.

vortex core polarities p_A and p_B. As shown in Ref. [23], we observe a narrow microwave signal only in the case when they are opposite, $p_A p_B = -1$, and when I_{dc} exceeds a threshold current $I_{th} \simeq 8$ to 11 mA depending on $H_\perp$. The spontaneous microwave emission branch at $I_{dc} = 20$ mA for which $p_A = +1$ and $p_B = -1$ is displayed in Fig. 1(c). The oscillation frequency linearly decreases with increasing $H_\perp$, as expected for a gyrotropic mode dominated by the thick layer vortex, whose polarity is antiparallel to the applied field [25]. The observed emission frequency, which decreases from 750 to 450 MHz as $H_\perp$ increases from −0.7 to 3 kOe, agrees well [23] with the expected gyrotropic frequency for the thick Py_B layer augmented with the contributions of the Oersted field [26,27] and of the dipolar coupling to the thin Py_A layer [28]. The boundaries of the frequency branch shown in Fig. 1(c) result from the combined action of $H_\perp$ and STT to reverse the vortex cores in the Py layers [29].

We now concentrate on the dependence of the generation linewidth on $H_\perp$, which is plotted in Fig. 2(a) using dark blue symbols (ΔF_1). It displays minima down to 40 kHz ($F_1/\Delta F_1 \simeq 19000$) and maxima up to 1 MHz ($F_1/\Delta F_1 \simeq 700$), i.e., a decrease of spectral purity by more than a factor 25 by changing $H_\perp$ from −0.7 [Fig. 1(a)] to −0.15 kOe [Fig. 1(b)]. We first note that the strong variations of the linewidth observed at $I_{dc} = 20$ mA cannot be attributed to changes of the nearly constant supercriticality ($I_{dc}/I_{th} \simeq 2$) or integrated power [0.32 pW at $H_\perp = -0.7$ kOe vs 0.4 pW at $H_\perp = -0.15$ kOe , see Figs. 1(a) and 1(b)]. The generation linewidth of a nonlinear auto-oscillator can be written as [17]

$$\Delta F_g = \frac{k_B T}{E_s}\frac{\Gamma_+}{2\pi}(1+\nu^2), \tag{1}$$

where k_B is the Boltzmann constant, T the temperature, E_s the energy stored in the auto-oscillation, Γ_+ the natural energy dissipation rate, and ν the nonlinear phase-amplitude coupling parameter. The latter is defined as $\nu = Np/\Gamma_p$, the dimensionless ratio between the nonlinear frequency shift N multiplied by the normalized oscillation power p and divided by the damping rate of amplitude fluctuations Γ_p [15].

Since the spectral linewidth ΔF_g depends quadratically on ν, the dependence of this parameter on $H_\perp$ should be evaluated. For this, we analyze the linewidth of the harmonics of the auto-oscillation signal. It was shown in Ref. [30] that the linewidth ΔF_n of the nth harmonics is related to the fundamental one (ΔF_1) by

$$\frac{1}{n^2} = \Delta F_1\left(\frac{1+\nu^2}{\Delta F_n} - \nu^2\frac{1-\exp(-2\Gamma_p/\Delta F_n)}{2\Gamma_p}\right). \tag{2}$$

We have plotted in Fig. 2(a) the evolution of $\Delta F_n/n^2$ ($n = 2$ to 4) together with the one of ΔF_1. It is clear from

this graph that independently of $H_\perp$, $\Delta F_n \simeq n^2 \Delta F_1$, which means that our STNO is quasi-isochronous and, from Eq. (2), that $\nu \simeq 0$ in the full field range. Therefore, one can also exclude that the strong variations of linewidth observed in Fig. 2(a) are due to some changes of ν with $H_\perp$. Moreover, we can estimate the generation linewidth from Eq. (1) when $\nu = 0$. For the vortex gyrotropic mode with angular frequency ω, $E_s = \frac{1}{2} G\omega X^2$, where $G = 2\pi L M_s/\gamma$ is the gyrovector and X the gyration radius of the core and $\Gamma_+ = \eta\alpha\omega$ [31]. For the thick Py_B layer ($L = 15$ nm), $M_s = 764\,\mathrm{emu\cdot cm^{-3}}$, $\gamma = 1.87\times10^7\,\mathrm{rad\cdot s^{-1}\,Oe^{-1}}$, and the damping coefficient $\alpha = 0.008$ were determined by mechanical ferromagnetic resonance [32], and the topological renormalization of damping is $\eta = 1.7$ [26]. From micromagnetic simulations [33], the radius of gyration under bias conditions close to the experimental ones is found to be $X \simeq 40\,\mathrm{nm}$ [corresponding to $p = (X/R)^2 \simeq 0.1$]. Hence, at room temperature, $k_B T/E_s \simeq 0.003$ and $\Gamma_+/(2\pi) = 9.5$ MHz, which yields $\Delta F_g = 29$ kHz, a value close to the narrow linewidth of 40 kHz observed at $H_{\mathrm{ext}} = -0.7$ kOe [Fig. 1(a)], which thus almost coincides with the intrinsic linewidth of our oscillator. In sum, the absence of nonlinear broadening and the large energy stored in the auto-oscillation in comparison to the thermal energy explain the low minimal values (< 100 kHz) of the linewidth in Fig. 2(a).

Before seeking further the origin of the variations of linewidth, we first investigate possible physical causes of quasi-isochronicity. Despite the fact that the nonlinearity ν of our STNO is nearly zero, it exhibits a large frequency tunability $dF/dI_{\mathrm{dc}} \simeq 7$ MHz/mA, see Fig. 2(b). This can be explained by the linear contribution of the Oersted field to the oscillation frequency. In fact, the tunability can be decomposed as follows:

$$\frac{dF}{dI_{\mathrm{dc}}} = \frac{\partial F}{\partial p}\frac{\partial p}{\partial I_{\mathrm{dc}}} + \frac{\partial F}{\partial I_{\mathrm{dc}}} = N\frac{\partial p}{\partial I_{\mathrm{dc}}} + A_{\mathrm{Oe}} I_{\mathrm{dc}}. \qquad (3)$$

In the vortex state, the Oersted field participates in the confinement potential of the vortex core [26,27], and for our STNO parameters, it is predicted to be about $A_{\mathrm{Oe}} \simeq 12.5$ MHz/mA. Therefore, a nonlinear frequency shift $N \neq 0$ is not required to obtain a large tuning sensitivity in Eq. (3). Here, the measured tunability is comparable with the one expected for the Oersted field alone. We attribute the somewhat smaller experimental value to the fact that the auto-oscillating mode does not only involve the thick Py layer, but also the thin one [23], which is not taken into account in the calculation of A_{Oe}.

For the gyrotropic mode, N is the sum of the nonlinearities N_{ms} and N_{Oe} of the magnetostatic and the Oersted field confinement potentials, respectively. An analytical model [34] predicts that the exact value of N_{ms} is positive and depends on the aspect ratio of the magnetic dot in the vortex state, as confirmed by recent micromagnetic simulations [27] and experiments [35]. On the contrary, N_{Oe} is negative when the vortex chirality is parallel to the Oersted field. Therefore, the two contributions can compensate each other (see Fig. 3 of Ref. [27]), using our STNO parameters $N = N_{\mathrm{ms}} + N_{\mathrm{Oe}} = 0$ for $I_{\mathrm{dc}} = 23$ mA. Experimentally, we find that $\nu \simeq 0$ is robust from 18 up to 25 mA by analyzing the linewidths of harmonics as in Fig. 2(a). By using Eq. (2), we can be more quantitative [30]: in the full window of field and current, we extract that $\nu < 0.5$ and that Γ_p ranges between 2 and 10 MHz. Hence, the intrinsically small N with respect to $\Gamma_p/p \simeq 10\Gamma_p$ in our STNO is probably responsible for $\nu < 0.5$ [36]. Moreover, as mentioned before, the auto-oscillating mode in our sample involves both the thick and thin vortex Py layers with opposite core polarities. Several nonconservative STT terms are thus involved in the dynamics [37], which could be another cause of quasi-isochronicity: micromagnetic simulations have indeed shown that such terms can substantially reduce the nonlinear phase-amplitude coupling [38].

To elucidate the linewidth broadenings observed in Fig. 2(a), it should be noticed that in addition to the gyrotropic mode dominated by the thick Py_B layer excited by STT, there is a gyrotropic mode dominated by the thin Py_A layer, which for $I_{\mathrm{dc}} > 0$ is overdamped by STT [37]. In order to probe this mode, we use a microwave antenna deposited on top of the sample, which produces a microwave field h_{rf} in the plane of the Py layers [16,32], and detect the dc voltage generated through the nanopillar when the vortex gyrotropic dynamics is excited at resonance by $h_{\mathrm{rf}} = 3.6$ Oe [39]. We have reported the measured resonant frequency associated to the thin layer vortex mode as a function of $H_\perp$ in Fig. 3(a) using red dots. The detailed analysis of the observed behavior is out of the scope of this Letter and will be reported separately. For the following demonstration, it is sufficient to use a linear approximation of it (red straight line). As expected, the gyrotropic mode frequency f dominated by Py_A is lower and has an opposite slope versus $H_\perp$ than the one F_1 dominated by Py_B, due to smaller thickness ($L_A < L_B$) and opposite core polarity ($p_A = +1 = -p_B$) [25]. We also note that the linewidth of this mode ranges between 80 and 100 MHz, which is about 8 times larger than its natural linewidth, in agreement with the increase of relaxation of the thin layer due to STT.

Using red tone lines in Fig. 3(a), we have plotted its harmonics $n = 2$ to 5 together with the measured fundamental frequency F_1 and harmonics F_2 of the auto-oscillation signal (blue dots). We have also reported in Figs. 3(b) and 3(c) the inverse generation linewidth (logarithmic scale) and the slope $-dF_1/dH_\perp$ of the oscillation frequency versus $H_\perp$, respectively. At magnetic fields where the frequencies of the auto-oscillating and overdamped modes are commensurable, $pF_1 = qf$ with $p, q \in \mathbb{N}$ [dashed vertical lines in Fig. 3(a)], a decrease of $-dF_1/dH_\perp$ concomitant with a decrease of the inverse

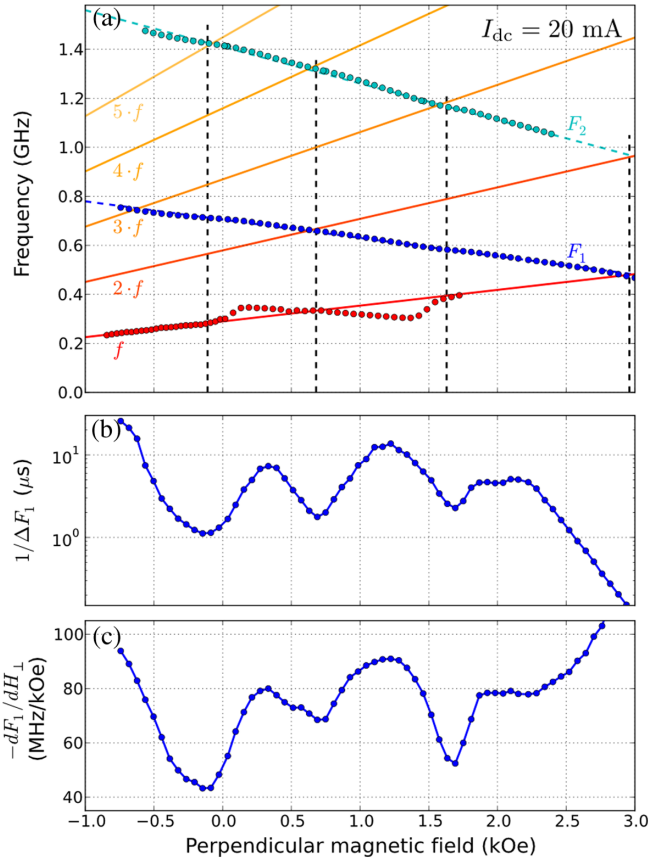

FIG. 3 (color online). (a) Blue dots: fundamental frequency F_1 and harmonics F_2 of the auto-oscillating mode dominated by the thick layer (vortex core polarity $p_B = -1$) as a function of $H_\perp$. Red dots: frequency f of the overdamped mode dominated by the thin layer (polarity $p_A = +1$). Red tone straight lines are guides to the eye and show successive harmonics of f. (b) Evolution of the inverse generation linewidth. (c) Slope of the oscillation frequency F_1 vs $H_\perp$.

linewidth is observed. We attribute this behavior to the interaction between the eigenmodes of the STNO [40]. When they cross each other, their frequency dispersions soften [41] and some energy can be transferred from the auto-oscillating mode to the overdamped mode. As a result, this additional channel of relaxation leads to a decrease of the coherence time of the auto-oscillation [this effect is not taken into account in Eq. (1), which was derived in a single mode approximation [15]]. Here, the dynamic dipolar interaction [42,43] is an obvious source of coupling between modes, but we stress that the dissipative STT terms at play in the double vortex configuration can also be important [37]. More theoretical work would be required to describe the multimode autonomous dynamics of our STNO [44]. Still, the main finding reported in Fig. 3 can be expressed in general terms, valid for all STNOs: the ratio of energy stored to energy lost in the system decreases when the auto-oscillating mode becomes degenerate with the overdamped mode. Since the coupling strength depends on the difference in energy between the modes, we emphasize that the STNO should better be operated under conditions where large frequency gaps exist between the auto-oscillating mode and other modes in the system [45–47].

In conclusion, we have presented a STNO based on coupled vortices having its spectral purity and tuning sensitivity uncorrelated, which is unusual for STNOs. We have demonstrated that it is quasi-isochronous in a broad range of bias conditions, which suppresses the most stringent cause of broadening and leads to high spectral purity. The latter reaches its intrinsic value $F/\Delta F > 10\,000$ only when the overdamped mode does not interact with the auto-oscillating mode. We have also pointed out that $\nu \simeq 0$ can be due to the compensation of the magnetostatic and Oersted field contributions to the nonlinear frequency shift in our device. Interestingly for applications, this does not prevent large tunability thanks to the linear contribution of the current induced Oersted field to the confinement potential of the vortex cores, which is general to vortex-based STNOs. In fact, our tunability is almost 8 MHz/mA at $H_\perp = -0.7$ kOe, the sweet point for spectral purity (see Fig. 2), which corresponds to about 200 times the linewidth in 1 mA.

We are greatly indebted to A. N. Slavin for fruitful discussions and for his support. This research was partly funded by the French ANR (Grant No. SPINNOVA ANR-11-NANO-0016) and the EU (FP7 Grant No. MOSAIC ICT-FP7-317950).

*gregoire.deloubens@cea.fr

[1] J. Slonczewski, J. Magn. Magn. Mater. **159**, L1 (1996).
[2] L. Berger, Phys. Rev. B **54**, 9353 (1996).
[3] S. I. Kiselev, J. C. Sankey, I. N. Krivorotov, N. C. Emley, R. J. Schoelkopf, R. A. Buhrman, and D. C. Ralph, Nature (London) **425**, 380 (2003).
[4] W. H. Rippard, M. R. Pufall, S. Kaka, S. E. Russek, and T. J. Silva, Phys. Rev. Lett. **92**, 027201 (2004).
[5] D. Houssameddine, U. Ebels, B. Delat, B. Rodmacq, I. Firastrau, F. Ponthenier, M. Brunet, C. Thirion, J.-P. Michel, L. Prejbeanu-Buda, M.-C. Cyrille, O. Redon, and B. Dieny, Nat. Mater. **6**, 447 (2007).
[6] P. K. Muduli, Y. Pogoryelov, S. Bonetti, G. Consolo, F. Mancoff, and J. Åkerman, Phys. Rev. B **81**, 140408 (2010).
[7] J. Zhu, J. A. Katine, G. E. Rowlands, Y.-J. Chen, Z. Duan, J. G. Alzate, P. Upadhyaya, J. Langer, P. K. Amiri, K. L. Wang, and I. N. Krivorotov, Phys. Rev. Lett. **108**, 197203 (2012).
[8] P. M. Braganca, B. A. Gurney, B. A. Wilson, J. A. Katine, S. Maat, and J. R. Childress, Nanotechnology **21**, 235202 (2010).
[9] K. Mizushima, K. Kudo, T. Nagasawa, and R. Sato, J. Phys. Conf. Ser. **266**, 012060 (2011).
[10] J.-G. Zhu and Y. Wang, IEEE Trans. Magn. **46**, 751 (2010).
[11] T. Shibata, R. Zhang, S. Levitan, D. Nikonov, and G. Bourianoff, in *Proceedings of the 13th International*

Workshop on Cellular Nanoscale Networks and Their Applications (CNNA) (IEEE, Piscataway, NJ, 2012), pp. 1–5.
[12] S. Petit-Watelot, J.-V. Kim, A. Ruotolo, R. M. Otxoa, K. Bouzehouane, J. Grollier, A. Vansteenkiste, B. V. de Wiele, V. Cros, and T. Devolder, Nat. Phys. **8**, 682 (2012).
[13] S. Urazhdin, P. Tabor, V. Tiberkevich, and A. Slavin, Phys. Rev. Lett. **105**, 104101 (2010).
[14] S. M. Mohseni, S. R. Sani, J. Persson, T. N. A. Nguyen, S. Chung, Y. Pogoryelov, P. K. Muduli, E. Iacocca, A. Eklund, R. K. Dumas, S. Bonetti, A. Deac, M. A. Hoefer, and J. Akerman, Science **339**, 1295 (2013).
[15] A. Slavin and V. Tiberkevich, IEEE Trans. Magn. **45**, 1875 (2009).
[16] A. Hamadeh, G. de Loubens, V. V. Naletov, J. Grollier, C. Ulysse, V. Cros, and O. Klein, Phys. Rev. B **85**, 140408 (2012).
[17] J.-V. Kim, V. Tiberkevich, and A. N. Slavin, Phys. Rev. Lett. **100**, 017207 (2008).
[18] M. W. Keller, M. R. Pufall, W. H. Rippard, and T. J. Silva, Phys. Rev. B **82**, 054416 (2010).
[19] M. Quinsat, D. Gusakova, J. F. Sierra, J. P. Michel, D. Houssameddine, B. Delaet, M.-C. Cyrille, U. Ebels, B. Dieny, L. D. Buda-Prejbeanu, J. A. Katine, D. Mauri, A. Zeltser, M. Prigent, J.-C. Nallatamby, and R. Sommet, Appl. Phys. Lett. **97**, 182507 (2010).
[20] V. S. Pribiag, I. N. Krivorotov, G. D. Fuchs, P. M. Braganca, O. Ozatay, J. C. Sankey, D. C. Ralph, and R. A. Buhrman, Nat. Phys. **3**, 498 (2007).
[21] A. Dussaux, B. Georges, J. Grollier, V. Cros, A. Khvalkovskiy, A. Fukushima, M. Konoto, H. Kubota, K. Yakushiji, S. Yuasa, K. Zvezdin, K. Ando, and A. Fert, Nat. Commun. **1**, 8 (2010).
[22] M. Manfrini, T. Devolder, J.-V. Kim, P. Crozat, N. Zerounian, C. Chappert, W. V. Roy, L. Lagae, G. Hrkac, and T. Schrefl, Appl. Phys. Lett. **95**, 192507 (2009).
[23] N. Locatelli, V. V. Naletov, J. Grollier, G. de Loubens, V. Cros, C. Deranlot, C. Ulysse, G. Faini, O. Klein, and A. Fert, Appl. Phys. Lett. **98**, 062501 (2011).
[24] V. Sluka, A. Kákay, A. M. Deac, D. E. Bürgler, R. Hertel, and C. M. Schneider, Phys. Rev. B **86**, 214422 (2012).
[25] G. de Loubens, A. Riegler, B. Pigeau, F. Lochner, F. Boust, K. Y. Guslienko, H. Hurdequint, L. W. Molenkamp, G. Schmidt, A. N. Slavin, V. S. Tiberkevich, N. Vukadinovic, and O. Klein, Phys. Rev. Lett. **102**, 177602 (2009).
[26] A. V. Khvalkovskiy, J. Grollier, A. Dussaux, K. A. Zvezdin, and V. Cros, Phys. Rev. B **80**, 140401 (2009).
[27] A. Dussaux, A. V. Khvalkovskiy, P. Bortolotti, J. Grollier, V. Cros, and A. Fert, Phys. Rev. B **86**, 014402 (2012).
[28] K. Y. Guslienko, K. S. Buchanan, S. D. Bader, and V. Novosad, Appl. Phys. Lett. **86**, 223112 (2005).
[29] N. Locatelli, A. E. Ekomasov, A. V. Khvalkovskiy, S. A. Azamatov, K. A. Zvezdin, J. Grollier, E. G. Ekomasov, and V. Cros, Appl. Phys. Lett. **102**, 062401 (2013).
[30] M. Quinsat, V. Tiberkevich, D. Gusakova, A. Slavin, J. F. Sierra, U. Ebels, L. D. Buda-Prejbeanu, B. Dieny, M.-C. Cyrille, A. Zelster, and J. A. Katine, Phys. Rev. B **86**, 104418 (2012).
[31] K. Y. Guslienko, Appl. Phys. Lett. **89**, 022510 (2006).
[32] V. V. Naletov, G. de Loubens, G. Albuquerque, S. Borlenghi, V. Cros, G. Faini, J. Grollier, H. Hurdequint, N. Locatelli, B. Pigeau, A. N. Slavin, V. S. Tiberkevich, C. Ulysse, T. Valet, and O. Klein, Phys. Rev. B **84**, 224423 (2011).
[33] A. V. Khvalkovskiy, J. Grollier, N. Locatelli, Y. V. Gorbunov, K. A. Zvezdin, and V. Cros, Appl. Phys. Lett. **96**, 212507 (2010).
[34] K. L. Metlov, J. Appl. Phys. **114**, 223908 (2013).
[35] O. V. Sukhostavets, B. Pigeau, S. Sangiao, G. de Loubens, V. V. Naletov, O. Klein, K. Mitsuzuka, S. Andrieu, F. Montaigne, and K. Y. Guslienko, Phys. Rev. Lett. **111**, 247601 (2013).
[36] P. M. Braganca, O. J. Lee, O. Ozatay, L. Liu, G. Finocchio, D. C. Ralph, and R. A. Buhrman, Appl. Phys. Lett. **102**, 252402 (2013).
[37] N. Locatelli, Ph.D. thesis, Université Paris Sud, 2012.
[38] D. Gusakova, M. Quinsat, J. F. Sierra, U. Ebels, B. Dieny, L. D. Buda-Prejbeanu, M.-C. Cyrille, V. Tiberkevich, and A. N. Slavin, Appl. Phys. Lett. **99**, 052501 (2011).
[39] S. Kasai, Y. Nakatani, K. Kobayashi, H. Kohno, and T. Ono, Phys. Rev. Lett. **97**, 107204 (2006).
[40] C. T. Boone, J. A. Katine, J. R. Childress, V. Tiberkevich, A. Slavin, J. Zhu, X. Cheng, and I. N. Krivorotov, Phys. Rev. Lett. **103**, 167601 (2009).
[41] B. Pigeau, C. Hahn, G. de Loubens, V. V. Naletov, O. Klein, K. Mitsuzuka, D. Lacour, M. Hehn, S. Andrieu, and F. Montaigne, Phys. Rev. Lett. **109**, 247602 (2012).
[42] S. Sugimoto, Y. Fukuma, S. Kasai, T. Kimura, A. Barman, and Y. C. Otani, Phys. Rev. Lett. **106**, 197203 (2011).
[43] P. S. Keatley, P. Gangmei, M. Dvornik, R. J. Hicken, J. Grollier, and C. Ulysse, Phys. Rev. Lett. **110**, 187202 (2013).
[44] O. Heinonen, P. Muduli, E. Iacocca, and J. Akerman, IEEE Trans. Magn. **49**, 4398 (2013).
[45] J. C. Sankey, I. N. Krivorotov, S. I. Kiselev, P. M. Braganca, N. C. Emley, R. A. Buhrman, and D. C. Ralph, Phys. Rev. B **72**, 224427 (2005).
[46] Q. Mistral, J.-V. Kim, T. Devolder, P. Crozat, C. Chappert, J. A. Katine, M. J. Carey, and K. Ito, Appl. Phys. Lett. **88**, 192507 (2006).
[47] J. F. Sierra, M. Quinsat, F. Garcia-Sanchez, U. Ebels, I. Joumard, A. S. Jenkins, B. Dieny, M.-C. Cyrille, A. Zeltser, and J. A. Katine, Appl. Phys. Lett. **101**, 062407 (2012).